RESEARCH ARTICLE
Open Access

Bridging One Health: Computational design of a multi-epitope messenger RNA vaccine for cross-species immunization against Nipah virus

Edward C. Banico[1], Ella Mae Joy S. Sira[1], Lauren Emily Fajardo[1], and Fredmoore L. Orosco[1,2,3]

1. Virology and Vaccine Research Program, Industrial Technology Development Institute, Department of Science and Technology, Taguig City, Philippines; 2. S&T Fellows Program, Department of Science and Technology, Taguig City, Philippines; 3. Department of Biology, College of Arts and Sciences, University of the Philippines Manila, Manila City, Philippines.

Corresponding author: Fredmoore L. Orosco, e-mail: florosco@up.edu.ph
Co-authors: ECB: ecbanico@alum.up.edu.ph, EMJSS: essira@alum.up.edu.ph, LEF: lfajardo@alum.up.edu.ph

Received: 31-07-2024, **Accepted:** 01-10-2024, **Published online:** 04-11-2024

doi: www.doi.org/10.14202/IJOH.2024.216-229 **How to cite this article:** Banico EC, Sira EMJS, Fajardo LE, and Orosco FL (2024) Bridging One Health: Computational design of a multi-epitope messenger RNA vaccine for cross-species immunization against Nipah virus, *Int. J. One Health*, 10(2): 216–229.

Abstract

Background and Aim: Nipah virus (NiV) poses a threat to human and animal health, particularly swine, which serve as primary vectors for human transmission. Despite its severe risks, no NiV vaccine currently exists for humans or animal hosts; thus, innovative vaccine development approaches that address cross-species transmission are required. This study was computationally designed to evaluate a multi-epitope messenger RNA (mRNA) vaccine targeting NiV for human and swine immunization.

Materials and Methods: B and T lymphocyte epitopes were identified from NiV structural proteins using multiple epitope prediction tools. All epitopes were linked to form a multi-epitope construct, and various adjuvant combinations were analyzed for physicochemical properties and immune simulation. Molecular docking and dynamics were employed to visualize the construct's interaction with a host immune receptor. Signal peptides were added to the construct, and mRNA sequences were generated using LinearDesign. The minimum free energies (MFEs) and codon adaptation indices (CAI) were used to select the final mRNA sequence of the vaccine construct.

Results: Computational tools predicted 10 epitopes within NiV structural proteins that can be recognized by human and swine immune receptors. The construct with β-defensin 2 adjuvant was selected as the final immunogenic region after showing favorable immunogenicity profiles and physicochemical properties. The final vaccine sequence had higher MFE and CAI compared to the BioNTech/Pfizer BNT162b2 and Moderna mRNA-1273 vaccines.

Conclusion: The multi-epitope mRNA vaccine designed in this study shows promising results as a potential NiV vaccine candidate. Further *in vivo* and *in vitro* studies are required to confirm the efficacy.

Keywords: computational design, cross-species immunization, messenger RNA vaccine, multi-epitope, Nipah virus.

Introduction

Nipah virus (NiV), a zoonotic virus of the *Paramyxoviridae* family, causes severe and fatal neurological diseases in humans [1]. The virus was first discovered in Malaysia in 1988 after reports of encephalitis cases and deaths related to neurological distress [1, 2]. In 2001–2019, around 400 NiV cases and 47 NiV-related deaths were reported sporadically in South and Southeast Asia [1]. At present, NiV vaccines are not available in the market. The sporadic nature of outbreaks limits the commercial viability of vaccines against the virus [3]. However, despite its infrequent outbreaks, the virus remains a significant threat to public health because of its high fatality rate [1, 4]. Various vaccines against NiV have been extensively explored [5, 6]; and among the promising platforms is messenger RNA (mRNA) vaccines. mRNA vaccines have been successful against zoonotic diseases such as Ebola [7], influenza [8], rabies [9], and Zika virus [10]. At present, the development of an mRNA vaccine for NiV is focused on the attachment glycoprotein (G) derived from closely related Hendra virus (HeV). Subunit vaccines using recombinant HeV-G proteins are protective against NiV [5, 11, 12]. However, the use of HeV-G mRNA for vaccination still requires design and delivery optimizations [13].

Immunoinformatics is crucial in several aspects of vaccine design and evaluation [14]. This computational approach uses bioinformatics tools and algorithms to rapidly screen potential vaccine candidates based on their predicted immunogenicity, allowing a comprehensive evaluation of potential vaccine designs. Advances in our understanding of the existing biological parallels between human and veterinary immunology have paved the way for the development

of cross-species vaccines [15]. A promising initiative for developing cross-species vaccines targeting the Rift Valley Fever virus has already begun [16]; and zoonotic pathogens such as NiV can also capitalize on this approach.

This study used immunoinformatics to design a multi-epitope mRNA vaccine targeting NiV for human and swine immunization. In designing a cross-species vaccine against NiV, this study used NiV proteins instead of the most commonly explored HeV proteins. This is based on the premise that NiV-specific proteins may provide specific and effective antigens against NiV infection [17, 18]. In addition to NiV G, fusion glycoprotein (F) was used as an antigen source in this study. The F protein is a structural protein that is equally important as the G protein in virion attachment to the host [19].

Materials and Methods

Ethical approval

The computational analysis performed in this study did not require ethical approval, as it did not involve human participants or animal subjects.

Study period and location

The study was conducted over a period of eight months, from February 2024 to September 2024. Research activities took place at the Advanced Device and Materials Testing Laboratory (ADMATEL) of the Department of Science and Technology (DOST), Bicutan, Taguig City, Philippines, where relevant resources and facilities were available for the analysis.

Protein retrieval

The full-length reference sequences of the NiV F and G proteins were retrieved from the National Center for Biotechnology Information (NCBI) database [20] (https://ncbi.nlm.nih.gov) in January 2024. The Basic Local Alignment Search Tool for Proteins (BLASTP) suite [21] (https://blast.ncbi.nlm.nih.gov/Blast.cgi) was used to retrieve G and F protein variants from the same virus using a query cover >90%, excluding models, non-redundant RefSeq proteins, and uncultured/environmental sample sequences. The alignment of the protein sequences was directly retrieved from the server and uploaded to the Protein Variability Server (PVS) [22] (https://imed.med.ucm.es/PVS). Highly conserved fragments were identified using Shannon's variability entropy (H) ≥1.0.

Epitope mapping

Linear B lymphocyte (LBL) epitope prediction

LBL epitopes were predicted using BepiPred 3.0 [23] (https://services.healthtech.dtu.dk/services/BepiPred-3.0), SVMTrip [24] (https://sysbio.unl.edu/SVMTriP/prediction.php), and ABCPred servers [25] (https://webs.iiitd.edu.in/raghava/abcpred). ABCPred was set at a threshold of 0.85, while the parameters from both BepiPred and SVMTrip were kept at default. Epitopes predicted by BepiPred, SVMTRip, and ABCPred were submitted to the LBTope server [26] (https://webs.iiitd.edu.in/raghava/lbtope) to assess the confidence of the prediction. Only epitopes with a probability ≥60% were considered in subsequent analyses.

Cytotoxic T lymphocyte (CTL) epitope prediction

NetMHCcons 1.1 [27] (https://services.healthtech.dtu.dk/services/NetMHCcons-1.1) was used to predict the CTL epitopes in humans. Twenty-five reference human leukocyte antigens (HLAs) [28] were used for the prediction, and a cut-off percentile rank (PR) ≤0.5 or half maximal inhibitory concentration ≤50 was set. NetMHCpan 4.1 [29] (https://services.healthtech.dtu.dk/services/NetMHCpan-4.1) was used to predict CTL epitopes in swine. Forty-five swine leukocyte antigens (SLAs) [30–33] were used for prediction, and a cutoff of PR ≤0.5 was set. NetCTLpan 1.1 [34] (https://services.healthtech.dtu.dk/services/NetCTLpan-1.1) was used to screen epitopes with efficient proteasomal cleavage and transporters associated with antigen processing transport. A cutoff value of PR ≤1 was set for screening. Prediction of CTL epitopes in humans and swine was restricted to 9-mer peptides.

Helper T lymphocyte (HTL) epitope prediction

NetMHCIIpan 4.3 [35] (https://services.healthtech.dtu.dk/services/NetMHCIIpan-4.3) was used to predict HTL epitopes in humans. Twenty-seven reference HLAs [36] were used for prediction, and a cutoff of PR ≤1 was set. Immune Epitope Database Analysis (IEDB) MHCII binding prediction [29] (https://tools.iedb.org/mhcii) was used to predict HTL epitopes in swine. Due to the absence of SLAs in the prediction server, 43 HLAs recognized as equivalents of SLAs [37] were used for prediction, and a cutoff of PR ≤10 was set. The prediction of HTL epitopes in humans and swine was restricted to 15-mer peptides. The predicted epitopes were evaluated for cytokine-inducing potential, specifically, tumor necrosis factor (TNF) α in TNFepitope [38] (https://webs.iiitd.edu.in/raghava/tnfepitope), interleukin-6 (IL6) in IL-6Pred [39] (https://webs.iiitd.edu.in/raghava/il6pred), and interferon (IFN) γ in IFNepitope [40] (https://webs.iiitd.edu.in/raghava/ifnepitope).

Physicochemical tests

The predicted epitopes were further evaluated for antigenicity using Vaxijen 2.0 [41] (https://ddg-pharmfac.net/vaxijen/VaxiJen/VaxiJen.html), allergenicity using AllerTOP v2.0 [42] (https://ddg-pharmfac.net/AllerTOP/feedback.py), toxicity using ToxinPred [43] (https://webs.iiitd.edu.in/raghava/toxinpred/multipletest.php), and solubility using the Innovagen peptide solubility calculator (https://pepcalc.com/peptide-solubility-calculator.php) using default parameters.

mRNA vaccine design

Epitopes derived from the same protein and occupying overlapping positions were fused into a consensus sequence. The KK peptide was used to connect

LBL epitopes, AAY peptide was used to connect CTL epitopes, and GPGPG peptide was used to connect HTL epitopes. The HEYGAEALERAG peptide was used to connect the three epitope groups. Linked epitopes were attached to three different adjuvants: truncated human β-defensin 2 (thβd2), truncated human β-defensin 3 (thβd3), and 50S ribosomal protein L7/L12 (50SrpL7/L12) using EAAAK peptide linker. The adjuvant-multi-epitope vaccine constructs were evaluated for their potential antigenicity using VaxiJen v2.0, allergenicity using AllerTOP v2.0, solubility using the Innovagen peptide solubility calculator, and stability using Expasy Protparam [44] (https://web.expasy.org/protparam). The host immune response profiles of the three adjuvant multi-epitope vaccine constructs were predicted using C-Immsim [45] (https://kraken.iac.rm.cnr.it/C-IMMSIM). Three injections of 1000 particles were applied at 1-84-168 time steps, and the simulation was run for 300 time steps. Graphs of antibody titers, IFN-γ concentration, population of B lymphocyte, and CTL and HTL populations induced by adjuvant multi-epitope vaccine constructs were compared. The adjuvant multi-epitope vaccine construct with the most favorable physicochemical properties and immune simulation profile was selected as the final immunogenic region of the NiV mRNA vaccine.

The tissue plasminogen activator (tPA) sequence was added to the N-terminus of the final immunogenic region of the NiV mRNA vaccine, and the MHC I-trafficking domain (MITD) sequence was added to its C-terminus. This represents the open reading frame (ORF) of the NiV mRNA vaccine. LinearDesign [46] (https://github.com/LinearDesignSoftware/LinearDesign) was used to generate the ORF RNA sequences. The codon adaptation indices (CAIs) of the RNA sequences were computed using the version 5 of the data analysis for molecular biology and evolution (DAMBE5) server [47] (http://dambe.bio.uottawa.ca/DAMBE/dambe.aspx). Several sequences were incorporated into the ORFs, including the human α globin (hαg) 5' untranslated region (UTR) and Kozak sequence into the N-terminal; and the hαg 3' UTR and a 120-length poly(A) sequence into the C-terminal. The RNAfold web server [48] (https://rna.tbi.univie.ac.at//cgi-bin/RNAWebSuite/RNAfold.cgi) was used to visualize the optimal secondary structure of the RNA sequences and compute their minimum free energies (MFEs). The Forna web server [49] (https://rna.tbi.univie.ac.at/forna) was used to highlight the 5′UTR and Kozak sequence regions within the RNA structures.

Two SARS-CoV-2 mRNA vaccine sequences (BioNTech/Pfizer BNT162b2 and Moderna mRNA-1273) were used as positive controls in the study. The sequences were retrieved [50], and their CAIs and MFEs were evaluated using the abovementioned servers and parameters. Due to the significant difference in the ORF length of the mRNA vaccine used in this study compared with the control, an adjusted MFE (AMFE) calculation was applied [51, 52]. This was computed by dividing the MFE by the sequence length and multiplying the result by 100. The RNA sequence with the closest CAI and AMFE to those of the controls was selected as the final sequence of the NiV mRNA vaccine.

Vaccine evaluation

Structures prediction

ColabFold v1.5.2-patch [53] in AlphaFold v2 [54] (https://colab.research.google.com/github/sokrypton/ColabFold/blob/main/AlphaFold2.ipynb) was used to predict the tertiary structure of the immunogenic region. Pdb100 was selected for template detection. The generated model was energy-minimized using Chimera 1.17.1 [55] (https://www.cgl.ucsf.edu/chimera/docindex.html) at 5000 steps of the steepest descent, and further refinement was performed using the GalaxyWEB Refine2 service [56] (https://galaxy.seoklab.org/cgi-bin/submit.cgi?type=REFINE2). The qualities of the refined models were assessed using the ERRAT [57] and PROCHECK [58] services in SAVES v6.0 (https://saves.mbi.ucla.edu). The model with the highest scores on the quality servers was used as the representative model of the tertiary structure of the immunogenic region.

Molecular docking and dynamics analyses

The tertiary structure of the immunogenic region was docked to the human toll-like receptor 4 (TLR4) structure. The SWISS-MODEL homology modeling server [59] (https://swissmodel.expasy.org) was used to generate the human TLR4 model using the crystal structure (PDB ID: 3FXI) downloaded from the RCSB Protein Data Bank [60] (https://rcsb.org) as the template. The key residues involved in the interaction of TLR4 with lipopolysaccharide, a known TLR4 agonist, were identified using the 'contacts' function of Chimera 1.17.1, applying a van der Waals radii overlap of ≥−0.40. ClusPro 2.0 [61] (https://cluspro.bu.edu/login.php) was used to forcibly dock the adjuvant of the immunogenic region to the identified key residues.

Coarse-grained molecular dynamics using the Southampton Interface and Reduction Algorithm for Hydrodynamics (SIRAH) force field [62] on GROMACS 2023.2 [63], (https://manual.gromacs.org/2023.2/download.html) was used to analyze the stability of the complexes. The systems were solvated in WatFour solvent [64] and neutralized with appropriate sodium and chloride ions. Energy minimization was performed to reach a maximum of 50,000 steps per steepest descent. The system was set to equilibrium at a temperature and pressure of 300 K and 1 bar, respectively. The Molecular Mechanics/Generalized Born Surface Area service of the HawkDock server [65] (https://cadd.zju.edu.cn/hawkdock/) was used to determine the overall binding free energy (ΔG) of the complex and the energy decomposition of all residues

of the immunogenic region and the TLR4-myeloid differentiation factor 2 (MD2) complex.

Results

Protein retrieval

The reference sequences of the NiV F (ID: NP 112026) and G (ID: NP 112027) proteins were downloaded from NCBI. These sequences were used as input data for retrieving all NiV protein variants, which were then subjected to conservation analysis. This analysis identified regions within proteins that remained consistent across different variants, thereby identifying potential sites suitable for epitope mapping. The conserved regions within proteins are shown in the variability plot in Figure-1.

Epitope mapping

LBL epitope prediction

BepiPred 3.0, SVMTrip, ABCPred, and LBTope predicted eight LBL epitopes within the NiV F and G proteins. Only three epitopes passed the tests for antigenicity, allergenicity, toxicity, and solubility. The final list of LBL epitopes is presented in Table-1. These epitopes are located within highly conserved regions of their respective protein sources.

CTL epitope prediction

NetMHCCons 1.1 predicted 138 epitopes with high binding affinities to at least one of 25 HLAs. Only 69 epitopes passed the antigenicity, allergenicity, toxicity, and solubility tests. Among these, four epitopes were predicted by NetMHCpan 4.1 to have high binding affinities to at least one of the 45 SLAs, indicating their potential to induce cross-species protection. The final list of CTL epitopes is presented in Table-2. These epitopes are located within highly conserved regions of their respective protein sources.

HTL epitope prediction

NetMHCIIpan 4.3 predicted 97 epitopes with high binding affinities to at least one of 27 HLAs. Only 26 epitopes passed the tests for antigenicity, allergenicity, toxicity, and solubility. Among these, 23 epitopes were identified by IEDB MHCII binding prediction to have high binding affinities to at least one of the 43 SLA-equivalent HLAs, indicating their potential to induce cross-species protection. Among these, only five epitopes elicited at least one NiV-associated cytokine. The final HTL epitopes are presented in Table-3. These epitopes are located within highly conserved regions of their respective protein sources.

mRNA vaccine design

A multi-epitope vaccine construct was designed by joining all predicted epitopes using KK, AAY, GPGPG, and HEYGAEALERAG peptide linkers. Three adjuvant-multi-epitope vaccine constructs were designed by incorporating thβd2, thβd3, and 50SrpL7/L12 adjuvants in the N-terminal of the multi-epitope vaccine construct, each linked by an EAAAK peptide. Tests for antigenicity, allergenicity, solubility, and stability of the adjuvant-multi-epitope vaccine constructs were conducted, and the results are presented in Table-4. Using C-ImmSim, antibody titers, IFN concentrations, and T and B cell populations were predicted after three immunizations with adjuvant multi-epitope vaccine constructs. The resulting immune simulation profiles are shown in Figure-2.

The three designs passed all physicochemical tests. The selection of the final vaccine construct was

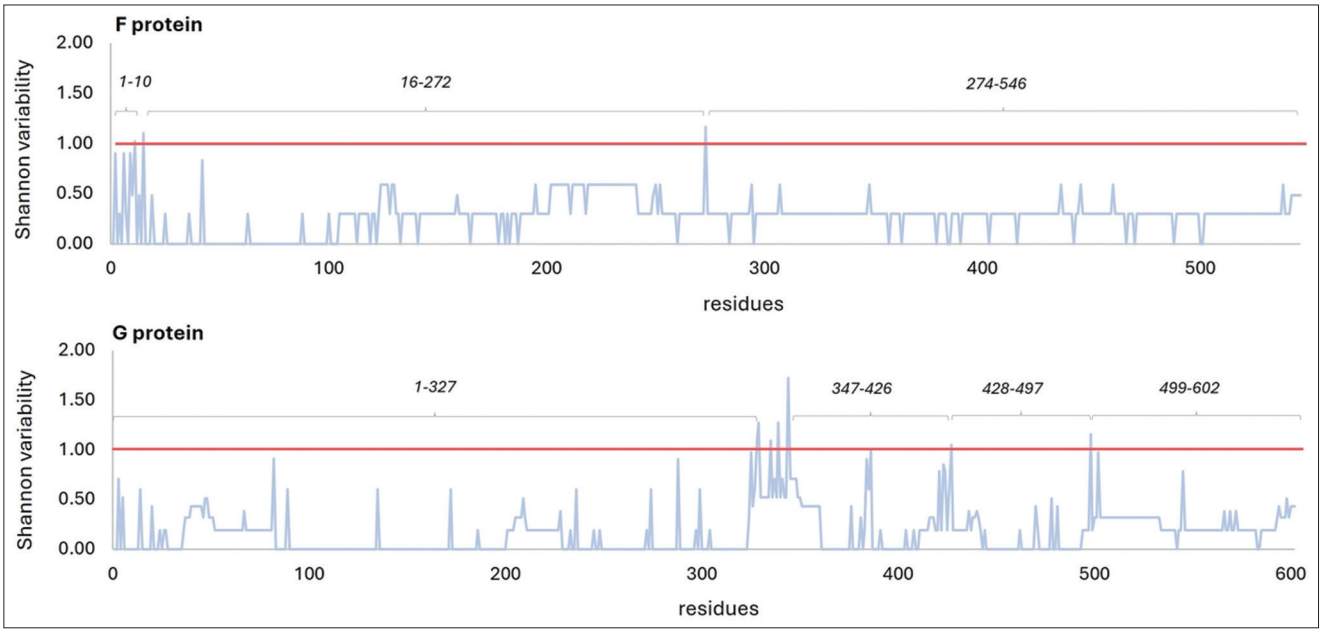

Figure-1: Variability plot of the fusion glycoprotein (F) and attachment glycoprotein (G) of the Nipah virus. Shannon variability values (Y-axis) were plotted against protein residues (X-axis). The red line indicates the variability threshold; residues below the red line are considered conserved. Conserved regions for each protein are indicated above the graphs in the italicized text.

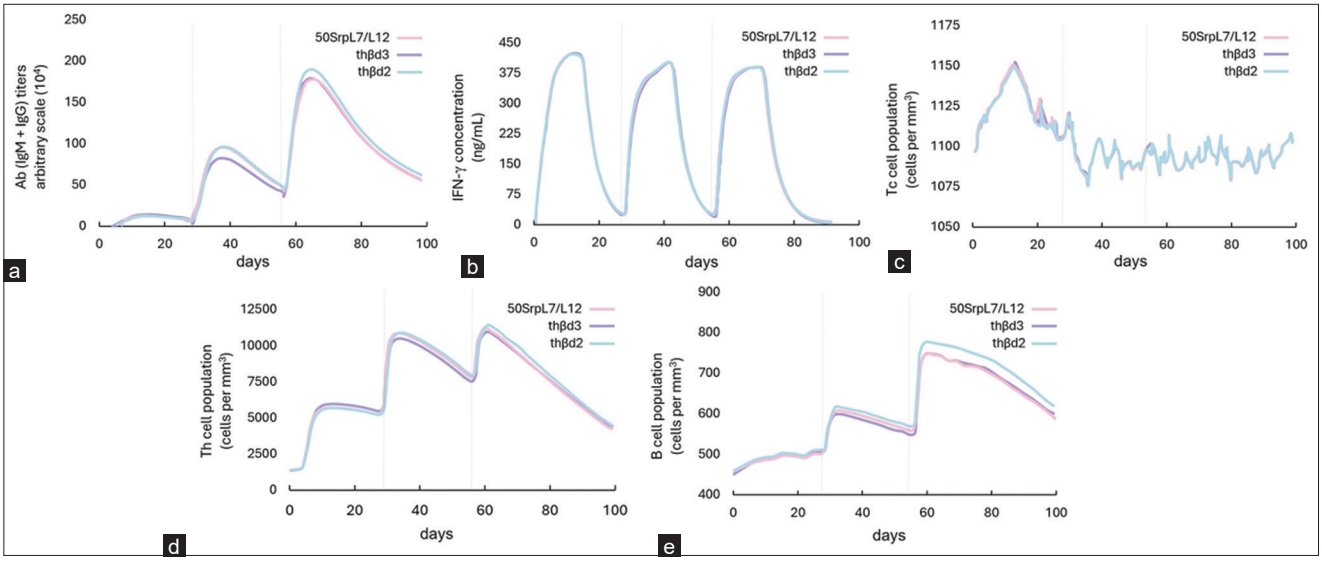

Figure-2: Immune simulation profile of the adjuvant-multi-epitope vaccine constructs at 0–4th and 4th–8th-week intervals. The gray line on the 28th day indicates the second immunization and the line on the 56th day indicates the third immunization. Graphs: (a) Antibody titers. (b) Interferon-γ concentration. (c) T-cytotoxic cell (Tc). (d) T-helper cell (TH) populations. (e) B lymphocyte populations.

Table-1: Linear B lymphocyte epitopes predicted from the fusion glycoprotein (F) and attachment glycoprotein (G) of the Nipah virus.

Epitopes	Protein source	LBTope percentage correct prediction
KKRNTYSRLEDRRVRPTSSGDLYY	F520-543	76.79
ESKKVRFENTASDKGKNPSKVIKSYYGTMDIKK	G4-36	75.02
EFKYNDSNCPIAECQYSKPENCRLSMGIRPNSH	G374-406	77.71

Table-2: Cytotoxic T lymphocyte epitopes predicted from the fusion glycoprotein (F) and attachment glycoprotein (G) of the Nipah virus.

Epitopes	Protein source	HLA covered	SLA covered
KIKSNPLTK	F47-55	A*03:01	1*12:01, 2*01:02
SVMENYKTR	F74-82	A*68:01	1*12:01, 2*01:02
SLDLALSKY	F198-206	A*01:01	1*02:01, 1*02:02, 1*04:01, 1*06:01, 1*07:01, 1*07:02, 1*08:01, 1*12:01, 1*13:01, 2*01:01, 2*01:02, 2*03:02, 2*04:01, 2*10:01, 2*10:02
KPKLISYTL	G199-207	B*07:02	1*11:01, 2*11:01, 3*05:01, 3*05:02, 3*05:03

HLAs=Human leukocyte antigens, SLAs=Swine leukocyte antigens

guided by the antigenicity score and immune response profile as determined by C-ImmSim simulations. The vaccine construct with thβd2 adjuvant demonstrated the highest antigenicity score at 0.66. This score was 8% higher than the antigenicity score of the vaccine construct with thβd3 adjuvant (0.61) and 20% higher than the vaccine construct with 50SrpL7/L12 adjuvant (0.53). In addition to the antigenicity scores, C-ImmSim simulations revealed that among the three vaccine constructs, the one with thβd2 adjuvant exhibited relatively higher simulation indices in certain tests. It demonstrated a 5%–7% increase in antibody titers on day 65, a 3% increase in B cell populations on day 60, and a 2%–4% increase in TH populations on day 60.

The tPA and MITD sequences were added to the N and C-terminus of the immunogenic region of the NiV mRNA vaccine, respectively. The immunogenic region incorporated by signal peptides constitutes the ORF. LinearDesign was used to generate a range of RNA sequences for the ORF. The list of mRNA vaccine candidates was finalized after adding UTRs and poly(A) tails to the ORF RNA sequences. Figure-3 presents the results of the evaluation of LinearDesign-generated RNA sequences for the NiV vaccine.

A $\lambda > 8$ for the LinearDesign-generated RNA sequence exhibited a higher CAI than did the two controls. However, even the least stable design ($\lambda > \infty$) recorded a higher AMFE than the two control designs (Figure-3a). This led to the selection of a CAI-optimal design as the final sequence for the NiV mRNA vaccine. Figure-3b shows the differences between the structures of the CAI-optimal and optimally stable designs for the NiV mRNA vaccine. The CAI-optimal design resulted in a relatively higher number of unpaired bases than the optimally stable design.

Although the structure of the 5′UTR of the final mRNA vaccine sequence (CAI-optimal design)

Table-3: Helper T lymphocyte epitopes predicted from the fusion glycoprotein (F) and attachment glycoprotein (G) of the Nipah virus.

Epitopes	Protein source	HLA covered	SLA covered
AVVKLQETAEKTVYV	F157-171	DP (A1*02:01-B1*14:01)	DR (B1*07:01), DR (B1*09:01)
T*FISFIIVEKKRNTY*	F511-526	DR (B1*13:02), DP (A1*02:01-B1*05:01)	DR (B1*03:01), DR (B1*08:01), DR (B1:11:01), DR (B1*13:01), DR (B1*14:01)
FISFIIVEKKRNTYS	F512-527	DR (B1*08:02), DR (B1*11:01)	DR (B1*03:01), DR (B1*08:01), DR (B1*11:01), DR (B1*12:01), DR (B1*13:01), DR (B1*14:01)
ISFIIVEKKRNTYSR	F513-528	DR (B1*13:02)	DR (B1*03:01), DR (B1*08:01), DR (B1*11:01), DR (B1*12:01), DR (B1*13:01), DR (B1*14:01)
VVNWRDNTVISRPGQ	G476-490	DR (B3*02:02)	DQ (A1*01:01-B1*04:01), DQ (A1*02:01-B1*04:01), DQ (A1*04:01-B1*04:01), DQ (A1*06:01-B1*04:01), DR (B1*03:01)

Italicized segments denote overlaps, indicating that they can be found in the same protein region. HLAs=Human leukocyte antigens, SLAs=Swine leukocyte antigens

Table-4: Physicochemical properties of adjuvant multi-epitope vaccine constructs with thβd2, thβd3, and 50S ribosomal protein L7/L12 (50SrpL7/L12) adjuvants.

Adjuvant-multi-epitope	Antigenicity score	Allergenicity	Solubility	Stability
thβd2-multi-epitope	0.66	Non-allergen	Soluble	Stable
thβd3-multi-epitope	0.61	Non-allergen	Soluble	Stable
50SrpL7/L12-multi-epitope	0.53	Non-allergen	Soluble	Stable

thβd2=Truncated human β-defensin 2, thβd3=Truncated human β-defensin 3

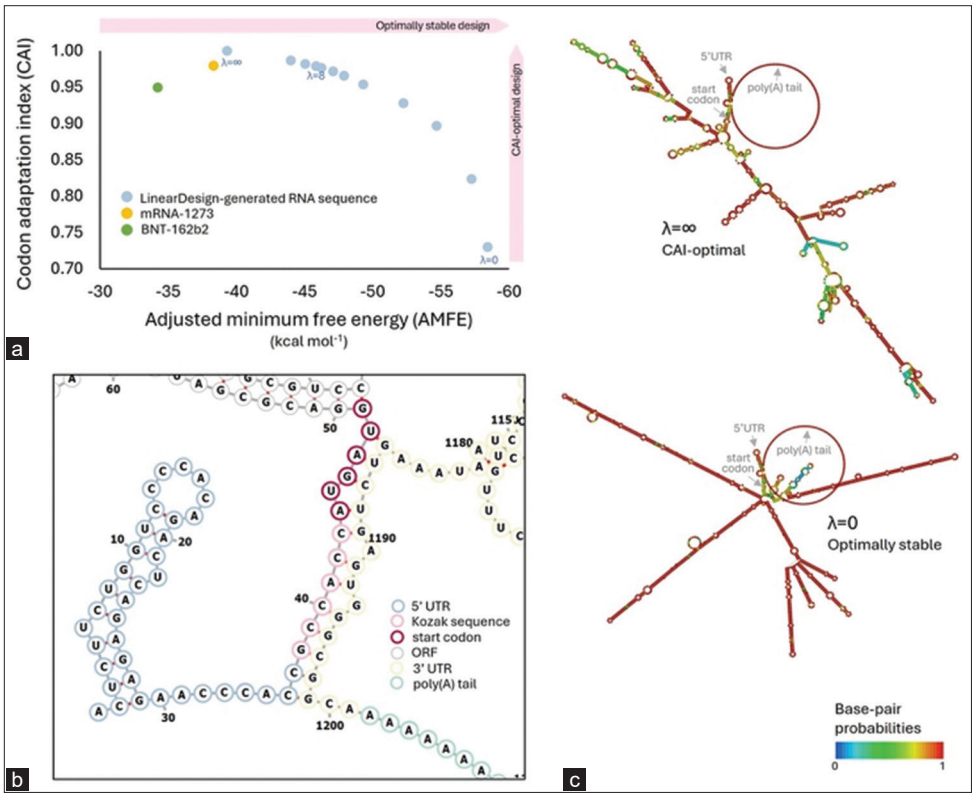

Figure-3: Evaluation of LinearDesign-generated RNA sequences for the NiV vaccine. (a) Two-dimensional visualization of the stability (represented by adjusted minimum free energy; X-axis) and codon optimality (represented by CAI; Y-axis) of the RNA sequences. λ being the weight assigned to codon optimality. Higher λ indicates higher weight in the CAI. (b) Secondary structures of the two mRNA vaccine designs for NiV. The optimal CAI design (top, λ = ∞) forms multiple loops with low pairing probabilities, whereas the optimally stable designs (bottom, λ = 0) formed helices with high pairing probabilities. (c) Closer view of the N-terminus of the final mRNA vaccine design (optimal-CAI design). NiV=Nipah virus, CAI=Codon adaptation indices, mRNA=Messenger RNA.

contained helices, as shown in Figure-3c, the base pair probabilities in this region were low. The components of the final multi-epitope mRNA vaccine against NiV are presented in Figure-4.

Vaccine evaluation

Structures prediction

Alphafold mutation predicted the tertiary structure of the immunogenic region. This structure was

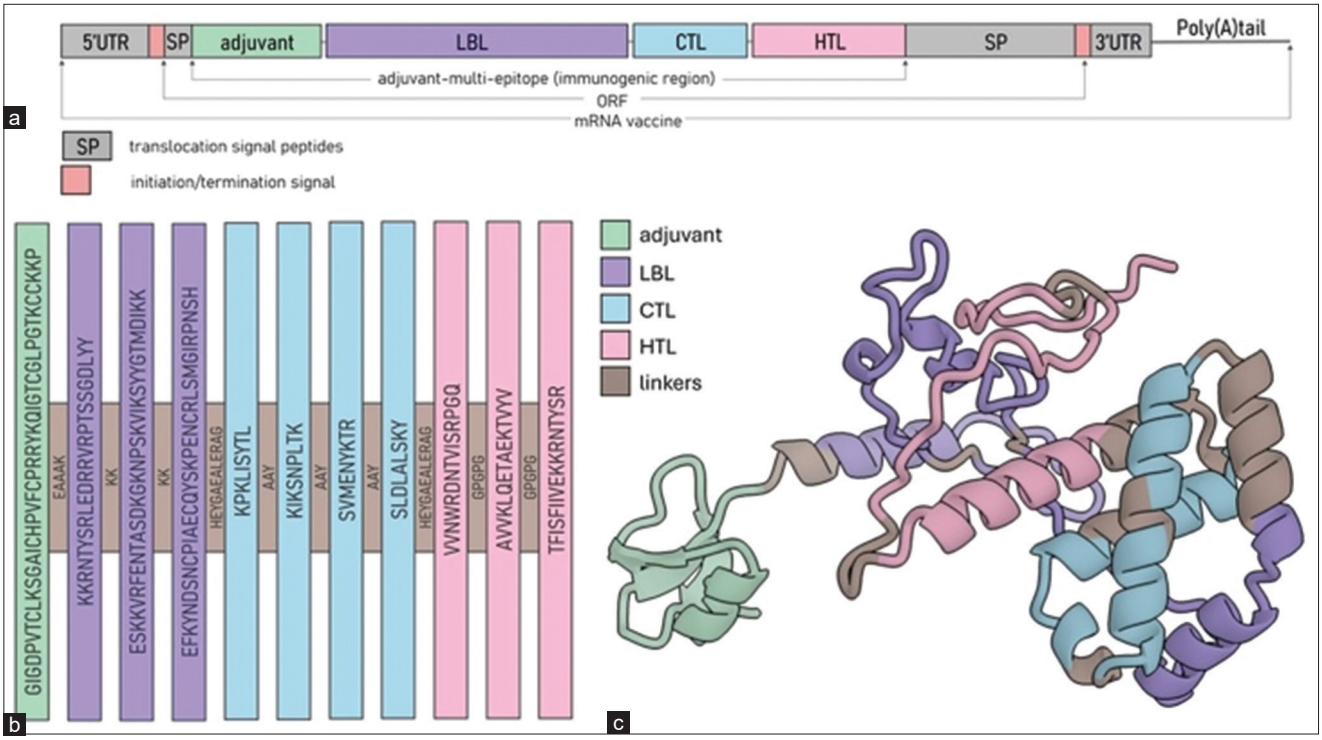

Figure-4: Components of the multi-epitope mRNA vaccine construct against Nipah virus. (a) Schematic of the full-length mRNA vaccine components. (b) Schematic diagram of the immunogenic region (adjuvant-multi-epitope). (c) Tertiary structure of the immunogenic region. mRNA=Messenger RNA.

energy minimized and refined using Chimera 1.17.1 and GalaxyRefine2, respectively. Among the 10 refined models generated, refined Model 2 had the highest overall quality factor for ERRAT (98.402) and the highest percentage of residues in the most favorable regions for PROCHECK (93.0). According to the server thresholds, these scores are considered the qualities of a high-resolution structure. Figure-4c shows the tertiary structural model of the immunogenic region.

Molecular docking and dynamics analyses

The immunogenic region was docked to the human TLR4 structure using ClusPro 2.0. Ten complexes were generated, but only in five complexes did the adjuvant region of the vaccine interact with the hydrophobic region of MD2 (Models 1, 2, 3, 6, and 7) (Figure-5). The overall binding free energy (ΔG) of these five complexes ranged from −74.5 (Model 2) to −125.55 kcal/mol (Model 3).

Figures-6a–c shows the binding free energies of the residues of the immunogenic region of the NiV mRNA vaccine and TLR4-MD2. Residues within MD2, such as S118 and S120, and within TLR4, including D238, R264, E270, D294, T296, T319, and R322, exhibited remarkably low negative free binding energies. Moreover, the interaction of the five complexes was observed to be stable, as indicated by the plateauing values of root mean square deviation (RMSD) over time (Figure-6d). The RMSD graphs show that after an initial equilibration period (approximately at 210 ns), the values for all five complexes reached a steady state and remained constant up to 300 ns.

Discussion

The results demonstrate the capacity of immunoinformatic to design and evaluate a multi-epitope mRNA vaccine against NiV. Most NiV multi-epitope vaccine designs published in the literature are subunit vaccines [66–71]. Multi-epitope mRNA vaccine designs are available [72, 73]. However, these studies focused exclusively on the immunogenic regions of mRNA without incorporating signal peptides and UTRs in the design and evaluation processes. For efficient mRNA delivery, it is crucial to consider these elements to enhance vaccine efficacy. This study represents the first multi-epitope mRNA vaccine design against NiV that incorporates these considerations.

The mRNA vaccine design of this study focused on two structural proteins, NiV F and G. Structural proteins were selected for epitope mapping because of their potential accessibility to the host immune system and because they are more likely to induce neutralizing antibodies [74]. Neutralizing antibodies bind to viral proteins [75], impeding their normal function and preventing viral infection [76, 77]. Both NiV F and G proteins are considered relevant protective antigens and targets for vaccine-elicited neutralizing antibodies [78]. Recent studies have identified antibodies that specifically recognize and bind to the G and F proteins of NiV [79, 80]. Focusing on these specific proteins ensures a targeted approach that enhances the likelihood of effective immune responses to the virus.

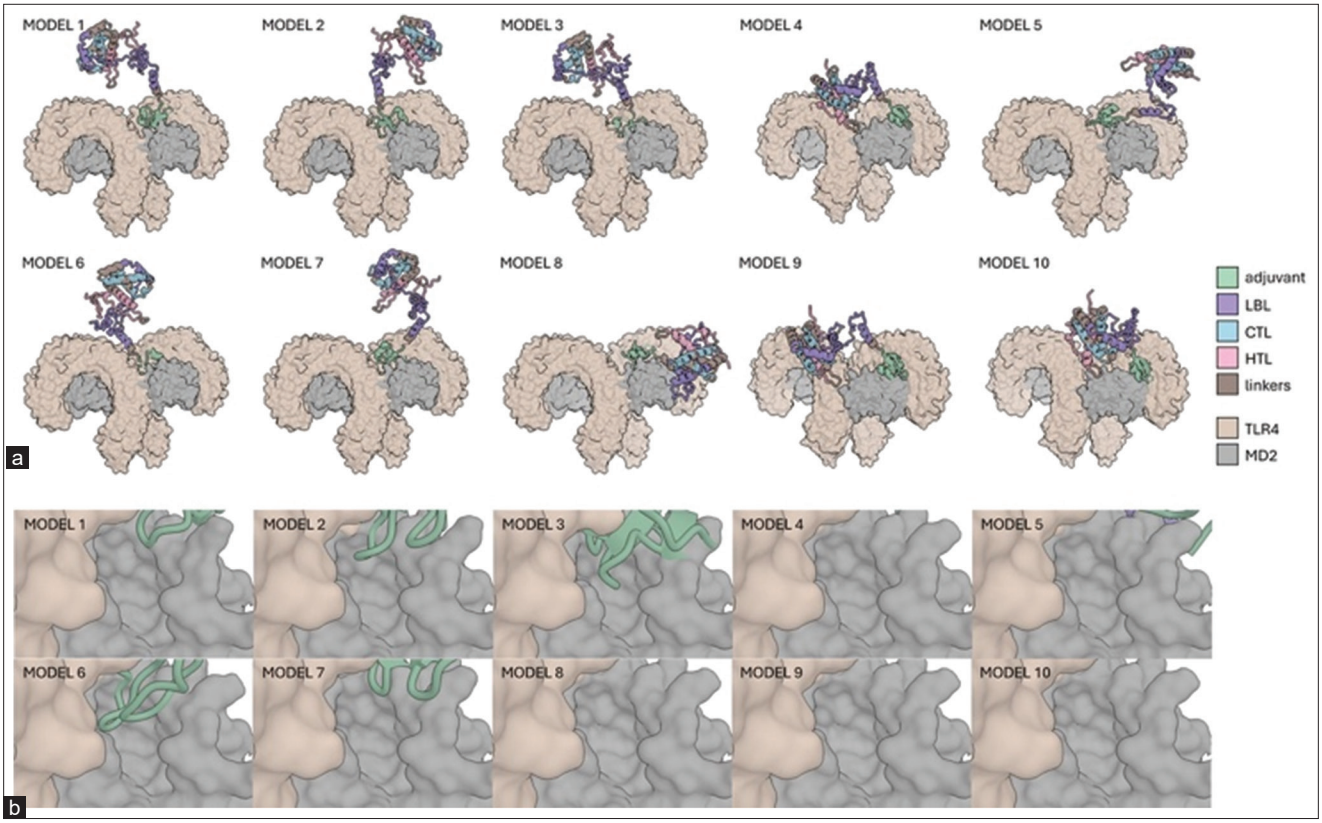

Figure-5: Molecular docking of the immunogenic region (adjuvant-multi-epitope) to TLR4-MD2. (a) Model of the docked complex. (b) Closer view of the hydrophobic region of MD2, where lipopolysaccharide, a known TLR4 agonist, binds. TLR4-MD2=Toll-like receptor 4-Myeloid differentiation factor 2.

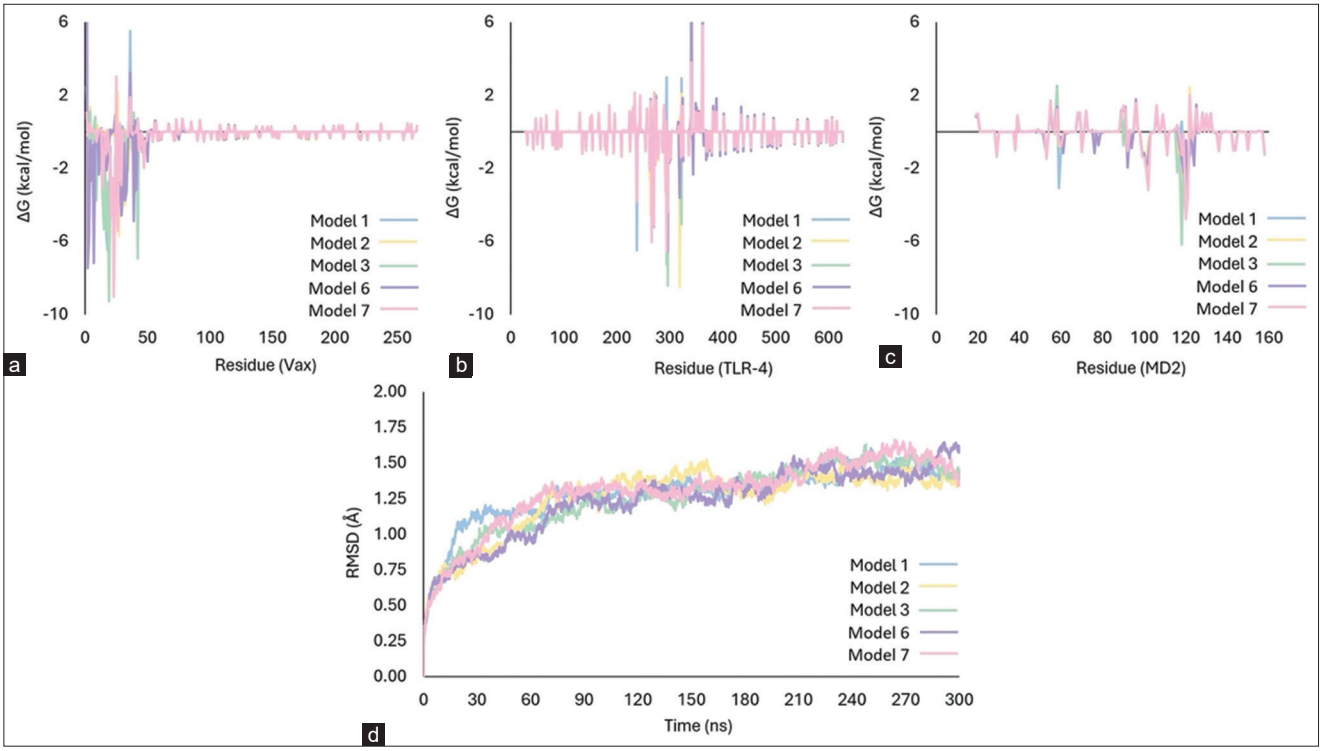

Figure-6: Binding free energies of the immunogenic region of the Nipah virus mRNA vaccine and the TLR4-MD2 residues. (a) Per-residue binding free energies of the immunogenic region. (b) Per-residue binding free energy of TLR4. (c) Per-residue binding free energy of MD2. (d) Root means square deviation graph of the complexes following 300 ns coarse-grained dynamics simulations. TLR4-MD2=Toll-like receptor 4-Myeloid differentiation factor 2, mRNA=Messenger RNA.

Three distinct components of the adaptive immune system were targeted in vaccine design: B cells, cluster of differentiation (CD) 8+ cytotoxic T cells, and CD4+ helper T cells. Each of these

components plays a crucial role in host defense against pathogens. B cells induce antibody-related functions and are activated by LBL epitopes. CD8+ cytotoxic T cells initiate cytotoxic responses and are activated by CTL epitopes. CD4+ helper T cells optimize the functions of B cells and CD8+ helper T cells and are activated by HTL epitopes. Screening of potential LBL, CTL, and HTL epitopes was guided by their potential for conservation, safety, and immunogenicity. As this study also aimed to design a vaccine that protects humans and swine, all epitope prediction servers were carefully selected to ensure their applicability across mammalian species. Moreover, human and swine major histocompatibility complex molecules have been used to identify immunogenic CTL and HTL epitopes.

The prediction of cytokine-inducing potential was also considered in the screening of HTL epitopes. In this study, the selection of HTL epitopes was limited to those capable of inducing at least one cytokine deemed essential for NiV control. The previous studies by Singh *et al*. [4] and Elvert *et al*. [81] on NiV infection in experimental animal models have revealed the induction of various cytokines in specific tissues. For instance, IL1α, IL6, IL8, granulocyte-colony stimulating factor, and the C-X-C motif chemokine 10 are induced in the airway epithelium, while TNFα and IL1β are induced in the central nervous system [4]. Furthermore, a significant level of IFNγ has been observed during *in vitro* infection of human and swine bronchial epithelial cells [81]. TNFα, IL6, and IFNγ, were the only cytokines considered in the study due to the availability of prediction servers specifically for these cytokines.

In this study, an adjuvant was incorporated into the multi-epitope vaccine construct. Adjuvants attract immune cells to the vaccination site, where they play essential roles in initiating, amplifying, and regulating the immune response [82, 83]. Various substances can serve as adjuvant components [84, 85], but this study focused on three adjuvants: hβd2, hβd3, and 50SrpL7/L12. These adjuvants have been incorporated in immunoinformatics-based multi-epitope subunit vaccine designs against NiV available in the literature [67, 68, 73]. The final vaccine construct with thβd2 adjuvant was selected due to its relatively higher antigenicity score and immune response profile in C-ImmSim compared with the other two designs (thβd3, and 50SrpL7/L12). The selected adjuvant, hβd2, like any other type of defensins, is commonly known for its antimicrobial properties [86], and its ability to exert immunomodulatory effects, particularly through cytokine induction [87, 88]. In general, defensins stimulate the TLR4 signaling pathway [85, 89, 90], enabling the production of pro-inflammatory cytokines such as IL-1, IL-6, and TNF-α [91], which are essential for the generation of memory T cells [92, 93]. Note that these cytokines are also highly expressed in NiV infection [4]. The adjuvant multi-epitope vaccine construct constituted the immunogenic region of the NiV vaccine.

Targeted molecular docking visualized possible interactions of hβd2 in the immunogenic region of the vaccine with the TLR4-MD2 complex. Highly negative free binding energies ranging from 74.5 to 125.55 kcal/mol were observed, corresponding to high binding affinity [94]. Moreover, the stability of the interactions between the immunogenic region of the vaccine and the TLR4-MD2 complexes was observed in molecular dynamics simulations. Stable interactions required at least 20–30 ns of constant RMSD following equilibration [95], a benchmark met by all five complexes in this study. The stability of these complexes indicates the presence of various conformations, suggesting that the vaccine can maintain a strong affinity for TLR4 across a range of structural states, ensuring an efficient immune response.

In this study, signal peptides and significant UTRs were incorporated into the design and evaluation of vaccines. A tPA signal peptide was added to the N-terminus, and an MITD sequence was added to the C-terminus of the immunogenic region. The tPA signal peptide was added to improve secretory protein expression, which is crucial for CD4+ helper T cell pathway activation and B cell epitope recognition [96]. On the other hand, MITD can translocate antigens into cellular compartments such as the ER and activate the CD8+ cytotoxic T cell pathway [97]. The immunogenic region containing signal peptides constitutes the ORF of the NiV vaccine.

The peptide sequence must be converted into mRNA to create an mRNA vaccine. This study employed LinearDesign, a novel approach that integrates considerations for both the CAI and folding dynamics [46] in mRNA vaccine design. CAI measures the extent to which a specific codon sequence aligns with the codon usage bias of the target organism to ensure efficient translation [98]. Folding dynamics or the mRNA secondary structure influence the stability of the molecule during translation [99]. The LinearDesign-generated ORF sequence exhibited superior CAI and secondary structure stability compared with two known mRNA vaccines, BioNTech/Pfizer BNT162b2 and Moderna mRNA-1273.

To complete the sequence of the NiV mRNA vaccine, several structures such as the UTR, initiation (Kozak sequence), termination signals, and poly(A) tails were added to the ORF sequence. This study attached the 5'UTR sequence of hαg. UTRs from human globin are among the most stable and efficiently translated mRNAs characterized [100–102], with estimated half-lives ranging from 24 to 60 h [103, 104]. This study also confirmed that the 5′UTR sequence lacks sequences for the start codon, ensuring the accuracy of protein synthesis [105]. This study incorporated two termination signals, hαg 3'UTR sequence, and poly(A) tail sequence 120 bases after the RNA sequence of the

ORF. A poly(A) tail length of 120 was found to be ideal for mRNA-based therapies [106].

Conclusion

This study successfully designed a safe, structurally stable, and immunogenic multi-epitope mRNA vaccine using immunoinformatics. Compared with conventional vaccine design, which relies heavily on extensive wet laboratory experiments, immunoinformatics-based approaches significantly reduce both the time and labor required for epitope screening. This expedited vaccine development process can effectively address the rapid emergence or re-emergence of numerous highly pathogenic infectious diseases.

This study adapted numerous benchmark studies from various server platforms to ensure the selection of the most effective tools for specific applications and minimize the pursuit of suboptimal vaccine candidates. Despite the efficiency of immunoinformatics, it has some notable limitations. The generalized mammalian models used by the servers do not specifically account for swine immunology. Therefore, there is a critical need to customize immunoinformatics tools and databases to suit the unique immunological profiles of target animal species. Tailoring these resources can enhance the accuracy and effectiveness of vaccine design for veterinary applications. In addition, it is crucial to emphasize that the structure of the mRNA vaccine used in this study serves as a preliminary framework for rigorous testing and validation. A comprehensive evaluation of all possible combinations and modifications of structural elements, such as UTRs and poly(A) tails, is also essential. This thorough testing will guide the final decision on the formulation to advance further development and potential deployment.

Authors' Contributions

ECB: Conceptualization, methodology, formal analysis, writing–original draft, and visualization. EMJSS: Methodology and writing–review and editing. LEF: Methodology and writing–review and editing. FLO: Conceptualization, supervision, and project administration. All authors have read and approved the final manuscript.

Acknowledgements

The authors are thankful to the Advanced Science and Technology Institute of the Department of Science and Technology (DOST-ASTI) Philippines for the use of their high-performance computing units to run molecular dynamics analyses; the Philippine Council for Agriculture, Aquatic, and Natural Resources Research and Development (PCAARRD) for their constant support, guidance, and provision of essential resources; and the staff of the Advanced Materials Testing Laboratory of the Department of Science and Technology (DOST-ADMATEL), who graciously provided their facility to conduct the research.

Competing Interests

The authors declare that they have no competing interests.

Publisher's Note

Veterinary World (Publisher of International Journal of One Health) remains neutral with regard to jurisdictional claims in published institutional affiliation.

References

1. Hauser, N., Gushiken, A.C., Narayanan, S., Kottilil, S. and Chua, J.V. (2021) evolution of Nipah virus infection: Past, present, and future considerations. *Trop. Med. Infect. Dis.*, 6(1): 24.
2. Chua, K.B., Bellini, W.J., Rota, P.A., Harcourt, B.H., Tamin, A., Lam, S.K., Ksiazek, T.G., Rollin, P.E., Zaki, S.R., Shieh, W., Goldsmith, C.S., Gubler, D.J., Roehrig, J.T., Eaton, B., Gould, A.R., Olson, J., Field, H., Daniels, P., Ling, A.E., Peters, C.J., Anderson, L.J. and Mahy, B.W. (2000) Nipah virus: A recently emergent deadly paramyxovirus. *Science*, 288(5470): 1432–1435.
3. McLean, R.K. and Graham, S.P. (2019) Vaccine development for Nipah virus infection in pigs. *Front. Vet. Sci*., 6: 16.
4. Singh, R.K., Dhama, K., Chakraborty, S., Tiwari, R., Natesan, S., Khandia, R., Munjal, A., Vora, K.S., Latheef, S.K., Karthik, K., Singh Malik, Y., Singh, R., Chaicumpa, W. and Mourya, D.T. (2019) Nipah virus: Epidemiology, pathology, immunobiology and advances in diagnosis, vaccine designing and control strategies - A comprehensive review. *Vet. Q.*, 39(1): 26–55.
5. Broder, C.C., Weir, D.L. and Reid, P.A. (2016) Hendra virus and Nipah virus animal vaccines. *Vaccine*, 34(30): 3525–3534.
6. Orosco F.L. (2023) Breaking the chains: Advancements in antiviral strategies to combat Nipah virus infections. *Int. J. One Health*, 9(2): 122–133.
7. Meyer, M., Huang, E., Yuzhakov, O., Ramanathan, P., Ciaramella, G. and Bukreyev, A. (2018) Modified mRNA-based vaccines elicit robust immune responses and protect guinea pigs from Ebola virus disease. *J. Infect. Dis.*, 217(3): 451-455.
8. Pardi, N., Parkhouse, K., Kirkpatrick, E., McMahon, M., Zost, S.J., Mui, B.L., Tam, Y.K., Karikó, K., Barbosa, C.J., Madden, T.D., Hope, M.J., Krammer, F., Hensley, S.E. and Weissman, D. (2018) Nucleoside-modified mRNA immunization elicits influenza virus hemagglutinin stalk-specific antibodies. *Nat. Commun*., 9(1): 3361.
9. Stokes, A., Pion, J., Binazon, O., Laffont, B., Bigras, M., Dubois, G., Blouin, K., Young, J.K., Ringenberg, M.A., Ben Abdeljelil, N., Haruna, J. and Rodriguez, L.A. (2020) Nonclinical safety assessment of repeated administration and biodistribution of a novel rabies self-amplifying mRNA vaccine in rats. *Regul. Toxicol. Pharmacol*., 113: 104648.
10. Richner, J.M., Himansu, S., Dowd, K.A., Butler, S.L., Salazar, V., Fox, J.M., Julander, J.G., Tang, W.W., Shresta, S., Pierson, T.C., Ciaramella, G. and Diamond, M.S. (2017) Modified mRNA vaccines protect against Zika virus infection. *Cell*, 168(6): 1114–1125.e10.
11. Pallister, J., Middleton, D., Wang, L.F., Klein, R., Haining, J., Robinson, R., Yamada, M., White, J., Payne, J., Feng, Y.R., Chan, Y.P. and Broder, C.C. (2011) A recombinant Hendra virus G glycoprotein-based subunit vaccine protects ferrets from lethal Hendra virus challenge. *Vaccine*, 29(34): 5623–5630.

12. Mire, C.E., Geisbert, J.B., Agans, K.N., Feng, Y.R., Fenton, K.A., Bossart, K.N., Yan, L., Chan, Y.P., Broder, C.C. and Geisbert, T.W. (2014) A recombinant Hendra virus G glycoprotein subunit vaccine protects nonhuman primates against Hendra virus challenge. *J. Virol*., 88(9): 4624–4631.
13. Amaya, M. and Broder, C.C. (2020) Vaccines to emerging viruses: Nipah and Hendra. *Annu. Rev. Virol.*, 7(1): 447–473.
14. Sira, E.M.J.S., Banico, E.C., Fajardo, L.E., Odchimar, N.M.O. and Orosco, F.L. (2024) Current strategies, advances, and challenges in multi-epitope subunit vaccine development for African swine fever virus. *Vet. Integr. Sci.*, 23(1): 2025011–2025012.
15. Warimwe, G.M., Francis, M.J., Bowden, T.A., Thumbi, S.M. and Charleston, B. (2021) Using cross-species vaccination approaches to counter emerging infectious diseases. *Nat. Rev. Immunol.*, 21(12): 815–822.
16. Warimwe, G.M., Gesharisha, J., Carr, B.V., Otieno, S., Otingah, K., Wright, D., Charleston, B., Okoth, E., Elena, L.G., Lorenzo, G., Ayman, E.B., Alharbi, N.K., Al-Dubaib, M.A., Brun, A., Gilbert, S.C., Nene, V. and Hill, A.V.S. (2016) Chimpanzee adenovirus vaccine provides multispecies protection against Rift Valley fever. *Sci. Rep.*, 6(1): 20617.
17. Guillaume, V., Contamin, H., Loth, P., Georges-Courbot, M.C., Lefeuvre, A., Marianneau, P., Chua, K.B., Lam, S.K., Buckland, R., Deubel, V. and Wild, T.F. (2004) Nipah virus: Vaccination and passive protection studies in a hamster model. *J. Virol.*, 78(2): 834–840.
18. Loomis, R.J., Stewart-Jones, G.B.E., Tsybovsky, Y., Caringal, R.T., Morabito, K.M., McLellan, J.S., Chamberlain, A.L., Nugent, S.T., Hutchinson, G.B., Kueltzo, L.A., Mascola, J.R. and Graham, B.S. (2020) Structure-based design of Nipah virus vaccines: A generalizable approach to paramyxovirus immunogen development. *Front. Immunol.*, 11: 842.
19. Byrne, P.O., Fisher, B.E., Ambrozak, D.R., Blade, E.G., Tsybovsky, Y., Graham, B. S., McLellan, J.S. and Loomis, R.J. (2023) Structural basis for antibody recognition of vulnerable epitopes on Nipah virus F protein. *Nat. Commun.*, 14(1): 1494.
20. Sayers, E.W., Bolton, E.E., Brister, J.R., Canese, K., Chan, J., Comeau, D.C., Connor, R., Funk, K., Kelly, C., Kim, S., Madej, T., Marchler-Bauer, A., Lanczycki, C., Lathrop, S., Lu, Z., Thibaud-Nissen, F., Murphy, T., Phan, L., Skripchenko, Y., Tse, T., Wang, J., Williams, R., Trawick, B.W., Pruitt, K.D. and Sherry, S.T. (2022) Database resources of the national center for biotechnology information. *Nucleic Acids Res*., 50(D1): D20–D26.
21. Boratyn, G.M., Camacho, C., Cooper, P.S., Coulouris, G., Fong, A., Ma, N., Madden, T.L., Matten, W.T., McGinnis, S.D., Merezhuk, Y., Raytselis, Y., Sayers, E.W., Tao, T., Ye, J. and Zaretskaya, I. (2013) BLAST: A more efficient report with usability improvements. *Nucleic Acids Res*., 41(W1): W29–W33.
22. Garcia-Boronat, M., Diez-Rivero, C.M., Reinherz, E.L. and Reche, P.A. (2008) PVS: A web server for protein sequence variability analysis tuned to facilitate conserved epitope discovery. *Nucleic Acids Res.*, 36: W35–W41.
23. Clifford, J.N., Høie, M.H., Deleuran, S., Peters, B., Nielsen, M. and Marcatili, P. (2022) BepiPred-3.0: Improved B-cell epitope prediction using protein language models. *Protein Sci*., 31(12): e4497.
24. Yao, B., Zhang, L., Liang, S. and Zhang, C. (2012) SVMTriP: A method to predict antigenic epitopes using support vector machine to integrate tri-peptide similarity and propensity. *PLoS One*, 7(9): e45152.
25. Saha, S. and Raghava, G.P.S. (2006) Prediction of continuous B-cell epitopes in an antigen using recurrent neural network. *Proteins*, 65(1): 40–48.
26. Singh, H., Gupta, S., Gautam, A. and Raghava, G.P.S. (2015) Designing B-Cell epitopes for immunotherapy and subunit vaccines. In: Houen, G., editor. Peptide Antibodies: Methods and Protocols. Springer, New York, p327–340.
27. Karosiene, E., Lundegaard, C., Lund, O. and Nielsen, M. (2012) NetMHCcons: A consensus method for the major histocompatibility complex class I predictions. *Immunogenetics*, 64(3): 177–186.
28. Weiskopf, D., Angelo, M.A., de Azeredo, E.L., Sidney, J., Greenbaum, J.A., Fernando, A.N., Broadwater, A., Kolla, R.V., De Silva, A.D., de Silva, A.M., Mattia, K.A., Doranz, B.J., Grey, H.M., Shresta, S., Peters, B. and Sette, A. (2013) Comprehensive analysis of dengue virus-specific responses supports an HLA-linked protective role for CD8+ T cells. *Proc. Natl. Acad. Sci. U S A*, 110(22): E2046–2053.
29. Reynisson, B., Alvarez, B., Paul, S., Peters, B. and Nielsen, M. (2020) NetMHCpan-4.1 and NetMHCIIpan-4.0: Improved predictions of MHC antigen presentation by concurrent motif deconvolution and integration of MS MHC eluted ligand data. *Nucleic Acids Res.*, 48(W1): W449–W454.
30. Buan, A.K.G., Reyes, N.A.L., Pineda, R.N.B. and Medina, P.M.B. (2022) *In silico* design and evaluation of a multi-epitope and multi-antigenic African swine fever vaccine. *ImmunoInformatics*, 8: 100019.
31. Ros-Lucas, A., Correa-Fiz, F., Bosch-Camós, L., Rodriguez, F. and Alonso-Padilla, J. (2020) Computational analysis of African swine fever virus protein space for the design of an epitope-based vaccine ensemble. *Pathogens*, 9(12): 1078.
32. Juan, A.K.A., Palma, K.M.C., Suarez, M.B. and Herrera-Ong, L.R. (2022) Immunoinformatics-based identification of highly conserved cytotoxic T-cell epitopes in polyprotein pp220 of African swine fever virus. *Biomed. Biotechnol. Res. J.*, 6: 319–325.
33. Simbulan, A.M., Banico, E.C., Sira, E.M.J.S., Odchimar, N.M.O. and Orosco, F.L. (2024) Immunoinformatics-guided approach for designing a pan-proteome multi-epitope subunit vaccine against African swine fever virus. *Sci. Rep.*, 14(1): 1354.
34. Stranzl, T., Larsen, M.V., Lundegaard, C. and Nielsen, M. (2010) NetCTLpan: Pan-specific MHC class I pathway epitope predictions. *Immunogenetics*, 62(6): 357–368.
35. Nilsson, J.B., Kaabinejadian, S., Yari, H., Kester, M.G.D., van Balen, P., Hildebrand, W.H. and Nielsen, M. (2023) Accurate prediction of HLA class II antigen presentation across all loci using tailored data acquisition and refined machine learning. *Sci. Adv.*, 9(47): eadj6367.
36. Greenbaum, J., Sidney, J., Chung, J., Brander, C., Peters, B. and Sette, A. (2011) Functional classification of Class II Human Leukocyte Antigen (HLA) molecules reveals seven different supertypes and a surprising degree of repertoire sharing across supertypes. *Immunogenetics*, 63(6): 325–335.
37. Techakriengkrai, N., Nedumpun, T., Golde, W.T. and Suradhat, S. (2021) Diversity of the swine leukocyte antigen Class I and II in commercial pig populations. *Front. Vet. Sci.*, 8: 637682.
38. Dhall, A., Patiyal, S., Choudhury, S., Jain, S., Narang, K. and Raghava, G.P.S. (2023) TNFepitope: A webserver for the prediction of TNF-α inducing epitopes. *Comput. Biol. Med.*, 160: 106929.
39. Dhall, A., Patiyal, S., Sharma, N., Usmani, S.S. and Raghava, G.P.S. (2021) Computer-aided prediction and design of IL-6 inducing peptides: IL-6 plays a crucial role in COVID-19. *Brief. Bioinform.*, 22(2): 936–945.
40. Dhanda, S.K., Vir, P. and Raghava, G.P. (2013) Designing of interferon-gamma inducing MHC class-II binders. *Biol. Direct.*, 8(1): 30.
41. Doytchinova, I.A. and Flower, D.R. (2007) VaxiJen: A server for prediction of protective antigens, tumour antigens and subunit vaccines. *BMC Bioinformatics*, 8(1): 4.
42. Dimitrov, I., Bangov, I., Flower, D.R. and Doytchinova, I.

(2014) AllerTOP v.2--a server for *in silico* prediction of allergens. *J. Mol. Model.*, 20(6): 2278.
43. Gupta, S., Kapoor, P., Chaudhary, K., Gautam, A., Kumar, R., Open Source Drug Discovery Consortium and Raghava, G.P.S. (2013) *In silico* approach for predicting toxicity of peptides and proteins. *PLoS One*, 8(9): e73957.
44. Gasteiger, E., Hoogland, C., Gattiker, A., Duvaud, S., Wilkins, M.R., Appel, R.D. and Bairoch, A. (2005) Protein identification and analysis tools on the ExPASy server. In: Walker, J.M., editor. The Proteomics Protocols Handbook. Humana Press: Totowa, NJ, p571–607.
45. Rapin, N., Lund, O., Bernaschi, M. and Castiglione, F. (2010) Computational immunology meets bioinformatics: The use of prediction tools for molecular binding in the simulation of the immune system. *PLoS One*, 5(4): e9862.
46. Zhang, H., Zhang, L., Lin, A., Xu, C., Li, Z., Liu, K., Liu, B., Ma, X., Zhao, F., Jiang, H., Chen, C., Shen, H., Li, H., Mathews, D.H., Zhang, Y. and Huang, L. (2023) Algorithm for optimized mRNA design improves stability and immunogenicity. *Nature*, 621(7978): 396–403.
47. Xia X. (2013) DAMBE5: A comprehensive software package for data analysis in molecular biology and evolution. *Mol. Biol. Evol.*, 30(7): 1720–1728.
48. Gruber, A.R., Lorenz, R., Bernhart, S.H., Neuböck, R. and Hofacker, I.L. (2008) The Vienna RNA Websuite. *Nucleic Acids Res.*, 36: W70–W74.
49. Kerpedjiev, P., Hammer, S. and Hofacker, I.L. (2015) Forna (force-directed RNA): Simple and effective online RNA secondary structure diagrams. *Bioinformatics*, 31(20): 3377–3379.
50. Jeong, D.E., McCoy, M., Artiles, K.L., Ilbay, O., Fire, A., Nadeau, K., Park, H.R., Betts, B., Boyd, S., Hoh, R. and Shoura, M. (2021) Assemblies of Putative SARS-CoV2-Spike-Encoding mRNA Sequences for Vaccines BNT-162b2 and mRNA-1273. Available from: https://www.semanticscholar.org/paper/assemblies-of-putative-sars-cov2-spike-encoding-for-jeong-mccoy/150b70589516b-969ce20fe83b9808478dd6f0e72. Retrieved on 09-05-2024.
51. Trotta, E. (2014) On the normalization of the minimum free energy of RNAs by sequence length. *PLoS One*, 9(11): e113380.
52. Zhang, B.H., Pan, X.P., Cox, S.B., Cobb, G.P. and Anderson, T.A. (2006) Evidence that miRNAs are different from other RNAs. *Cell. Mol. Life Sci.*, 63(2): 246–254.
53. Mirdita, M., Schütze, K., Moriwaki, Y., Heo, L., Ovchinnikov, S. and Steinegger, M. (2022) ColabFold: Making protein folding accessible to all. *Nat. Methods*, 19(6): 679–682.
54. Jumper, J., Evans, R., Pritzel, A., Green, T., Figurnov, M., Ronneberger, O., Tunyasuvunakool, K., Bates, R., Žídek, A., Potapenko, A., Bridgland, A., Meyer, C., Kohl, S.A.A., Ballard, A.J., Cowie, A., Romera-Paredes, B., Nikolov, S., Jain, R., Adler, J., Back, T., Petersen, S., Reiman, D., Clancy, E., Zielinski, M., Steinegger, M., Pacholska, M., Berghammer, T., Bodenstein, S., Silver, D., Vinyals, O., Senior, A.W., Kavukcuoglu, K., Kohli, P. and Hassabis, D. (2021) Highly accurate protein structure prediction with AlphaFold. *Nature*, 596(7873): 583–589.
55. Pettersen, E.F., Goddard, T.D., Huang, C.C., Couch, G.S., Greenblatt, D.M., Meng, E.C. and Ferrin, T.E. (2004) UCSF chimera--a visualization system for exploratory research and analysis. *J. Comput. Chem.*, 25(13): 1605–1612.
56. Heo, L., Park, H. and Seok, C. (2013) GalaxyRefine: Protein structure refinement driven by side-chain repacking. *Nucleic Acids Res*., 41: W384–W388.
57. Colovos, C. and Yeates, T.O. (1993) Verification of protein structures: Patterns of nonbonded atomic interactions. *Protein Sci*., 2(9): 1511–1519.
58. Laskowski, R.A., MacArthur, M.W., Moss, D.S. and Thornton, J.M. (1993) PROCHECK: A program to check the stereochemical quality of protein structures. *J. Appl. Crystallogr*., 26(2): 283–291.
59. Waterhouse, A., Bertoni, M., Bienert, S., Studer, G., Tauriello, G., Gumienny, R., Heer, F.T., de Beer, T.A.P., Rempfer, C., Bordoli, L., Lepore, R. and Schwede, T. (2018) SWISS-MODEL: Homology modelling of protein structures and complexes. *Nucleic Acids Res.*, 46(W1): W296–W303.
60. Berman, H.M., Westbrook, J., Feng, Z., Gilliland, G., Bhat, T.N., Weissig, H., Shindyalov, I.N. and Bourne, P.E. (2000) The protein data bank. *Nucleic Acids Res*., 28(1): 235–242.
61. Kozakov, D., Hall, D.R., Xia, B., Porter, K.A., Padhorny, D., Yueh, C., Beglov, D. and Vajda, S. (2017) The ClusPro web server for protein-protein docking. *Nat. Protoc.*, 12(2): 255–278.
62. Klein, F., Soñora, M., Helene Santos, L., Nazareno Frigini, E., Ballesteros-Casallas, A., Rodrigo Machado, M. and Pantano, S. (2023) The SIRAH force field: A suite for simulations of complex biological systems at the coarse-grained and multiscale levels. *J. Struct. Biol.*, 215(3): 107985.
63. Abraham, M.J., Murtola, T., Schulz, R., Páll, S., Smith, J.C., Hess, B. and Lindahl, E. (2015) GROMACS: High performance molecular simulations through multi-level parallelism from laptops to supercomputers. *SoftwareX*, 1: 19–25.
64. Darre, L., Machado, M.R., Dans, P.D., Herrera, F.E. and Pantano, S. (2010) Another coarse grain model for aqueous solvation: WAT FOUR? *J. Chem. Theory Comput.*, 6(12): 3793–3807.
65. Hou, T., Wang, J., Li, Y. and Wang, W. (2011) Assessing the performance of the MM/PBSA and MM/GBSA methods. 1. The accuracy of binding free energy calculations based on molecular dynamics simulations. *J. Chem. Inf. Model.*, 51(1): 69–82.
66. Majee, P., Jain, N. and Kumar, A. (2021) Designing of a multi-epitope vaccine candidate against Nipah virus by *in silico* approach: A putative prophylactic solution for the deadly virus. *J. Biomol. Struct. Dyn.*, 39(4): 1461–1480.
67. Srivastava, S., Verma, S., Kamthania, M., Saxena, A.K., Pandey, K.C., Pande, V. and Kolbe, M. (2023) Exploring the structural basis to develop efficient multi-epitope vaccines displaying interaction with HLA and TAP and TLR3 molecules to prevent NIPAH infection, a global threat to human health. *PLoS One*, 18(3): e0282580.
68. Raju, S., Sahoo, D. and Bhari, V.K. (2021) *In-silico* design of multi-epitope vaccine against Nipah virus using immunoinformatics approach. *J. Pure Appl. Microbiol.*, 15(1): 212–231.
69. Ojha, R., Pareek, A., Pandey, R.K., Prusty, D. and Prajapati, V.K. (2019) Strategic development of a next-generation multi-epitope vaccine to prevent Nipah virus zoonotic infection. *ACS Omega*, 4(8): 13069–13079.
70. Kumar, A., Misra, G., Mohandas, S. and Yadav, P.D. (2024) Multi-epitope vaccine design using *in silico* analysis of glycoprotein and nucleocapsid of NIPAH virus. *PLoS one*, 19(5): e0300507.
71. Shahab, M., Iqbal, M.W., Ahmad, A., Alshabrmi, F.M., Wei, D.Q., Khan, A. and Zheng, G. (2024) Immunoinformatics-driven *in silico* vaccine design for Nipah virus (NPV): Integrating machine learning and computational epitope prediction. *Comput. Biol. Med.*, 170: 108056.
72. Rahman, M.M., Puspo, J.A., Adib, A.A., Hossain, M.E., Alam, M.M., Sultana, S., Islam, A., Klena, J.D., Montgomery, J.M., Satter, S.M., Shirin, T. and Rahman, M.Z. (2022) An immunoinformatics prediction of novel multi-epitope vaccines candidate against surface antigens of Nipah virus. *Int. J. Pept. Res. Ther.*, 28(4): 123.
73. Albutti, A. (2023) An integrated multi-pronged reverse vaccinology and biophysical approaches for identification of potential vaccine candidates against Nipah virus. *Saudi*

Pharm. J., 31(12): 101826.
74. Murin, C.D., Wilson, I.A. and Ward, A.B. (2019) Antibody responses to viral infections: A structural perspective across three different enveloped viruses. *Nat. Microbiol.* 4(5): 734–747.
75. Ahmed, S., Parthasarathy, D., Newhall, R., Picard, T., Aback, M., Ratnapriya, S., Arndt, W., Vega-Rodriguez, W., Kirk, N.M., Liang, Y. and Herschhorn, A. (2023) Enhancing anti-viral neutralization response to immunization with HIV-1 envelope glycoprotein immunogens. *Npj Vaccines*, 8(1): 181.
76. Burton, D.R. (2023) Antiviral neutralizing antibodies: From *in vitro* to *in vivo* activity. *Nat. Rev. Immunol.*, 23(11): 720–734.
77. Ali, M. G., Zhang, Z., Gao, Q., Pan, M., Rowan, E.G. and Zhang, J. (2020) Recent advances in therapeutic applications of neutralizing antibodies for virus infections: An overview. *Immunol. Res.*, 68(6): 325–339.
78. Loomis, R.J., DiPiazza, A.T., Falcone, S., Ruckwardt, T.J., Morabito, K.M., Abiona, O.M., Chang, L.A., Caringal, R.T., Presnyak, V., Narayanan, E., Tsybovsky, Y., Nair, D., Hutchinson, G.B., Stewart-Jones, G.B.E., Kueltzo, L.A., Himansu, S., Mascola, J.R., Carfi, A. and Graham, B.S. (2021) Chimeric Fusion (F) and Attachment (G) glycoprotein antigen delivery by mRNA as a candidate Nipah vaccine. *Front. Immunol.*, 12: 772864.
79. Dang, H.V., Chan, Y.P., Park, Y.J., Snijder, J., Da Silva, S.C., Vu, B., Yan, L., Feng, Y.R., Rockx, B., Geisbert, T.W., Mire, C.E., Broder, C.C. and Veesler, D. (2019) An antibody against the F glycoprotein inhibits Nipah and Hendra virus infections. *Nat. Struct. Mol. Biol*., 26(10): 980–987.
80. Dang, H.V., Cross, R.W., Borisevich, V., Bornholdt, Z.A., West, B.R., Chan, Y.P., Mire, C.E., Da Silva, S.C., Dimitrov, A.S., Yan, L., Amaya, M., Navaratnarajah, C. K., Zeitlin, L., Geisbert, T.W., Broder, C.C. and Veesler, D. (2021) Broadly neutralizing antibody cocktails targeting Nipah virus and Hendra virus fusion glycoproteins. *Nat. Struct. Mol. Biol*., 28(5): 426–434.
81. Elvert, M., Sauerhering, L. and Maisner, A. (2020) Cytokine induction in Nipah virus-infected primary human and porcine bronchial epithelial cells. *J. Infect. Dis.*, 221(Suppl 4): S395–S400.
82. Orosco, F L. and Espiritu, L.M. (2024) Navigating the landscape of adjuvants for subunit vaccines: Recent advances and future perspectives. *Int. J. Appl. Pharm*., 16(1): 18–32.
83. Sira, E.M.J.S., Banico, E.C., Odchimar, N.M.O., Fajardo, L.E., Fremista, F.F. Jr., Refuerzo, H.A.B., Dictado, A.P.A. and Orosco, F.L. (2024) Immunoinformatics approach for designing a multiepitope subunit vaccine against porcine epidemic diarrhea virus genotype IIA spike protein. *Open Vet. J.*, 14(5): 1224–1224.
84. Zhao, T., Cai, Y., Jiang, Y., He, X., Wei, Y., Yu, Y. and Tian, X. (2023) Vaccine adjuvants: mechanisms and platforms. *Signal Transduct. Target. Ther.*, 8(1): 283.
85. Pulendran, B., Arunachalam, P.S. and O'Hagan, D. T. (2021) Emerging concepts in the science of vaccine adjuvants. *Nat. Rev. Drug Discov.*, 20(6): 454–475.
86. Gao, X., Ding, J., Liao, C., Xu, J., Liu, X. and Lu, W. (2021) Defensins: The natural peptide antibiotic. *Adv. Drug Deliv. Rev.*, 179: 114008.
87. Semple, F. and Dorin, J.R. (2012) β-Defensins: Multifunctional modulators of infection, inflammation and more? *J. Innate Immun.*, 4(4): 337–348.
88. Pivarcsi, A., Nagy, I., Koreck, A., Kis, K., Kenderessy-Szabo, A., Szell, M., Dobozy, A. and Kemeny, L. (2005) Microbial compounds induce the expression of pro-inflammatory cytokines, chemokines and human beta-defensin-2 in vaginal epithelial cells. *Microbes Infect*., 7(9): 1117–1127.
89. Biragyn, A., Ruffini, P.A., Leifer, C.A., Klyushnenkova, E., Shakhov, A., Chertov, O., Shirakawa, A.K., Farber, J.M., Segal, D.M., Oppenheim, J.J. and Kwak, L.W. (2002) Toll-like receptor 4-dependent activation of dendritic cells by beta-defensin 2. *Science*, 298(5595): 1025–1029.
90. Bolhassani, A., Talebi, S. and Anvar, A. (2017) Endogenous and exogenous natural adjuvants for vaccine development. *Mini Rev. Med. Chem.*, 17(15): 1442–1456.
91. Kim, J., Yang, Y.L., Jang, S.H. and Jang, Y.S. (2018) Human β-defensin 2 plays a regulatory role in innate antiviral immunity and is capable of potentiating the induction of antigen-specific immunity. *Virol. J.*, 15(1): 124.
92. Yang, D., Chen, Q., Chertov, O. and Oppenheim, J.J. (2000) Human neutrophil defensins selectively chemoattract naive T and immature dendritic cells. *J. Leukoc. Biol.*, 68(1): 9–14.
93. Yang, D., Biragyn, A., Kwak, L.W. and Oppenheim, J.J. (2002) Mammalian defensins in immunity: More than just microbicidal. *Trends Immunol.*, 23(6): 291–296.
94. Du, X., Li, Y., Xia, Y.L., Ai, S.M., Liang, J., Sang, P., Ji, X.L. and Liu, S.Q. (2016) Insights into protein-ligand interactions: Mechanisms, models, and methods. *Int. J. Mol. Sci.*, 17(2): 144.
95. Macalalad, M.A.B. and Orosco, F.L. (2024) *In silico* identification of multi-target inhibitors from medicinal fungal metabolites against the base excision repair pathway proteins of African swine fever virus. *RSC Adv*., 14(14): 10039–10055.
96. Wang, J.Y., Song, W.T., Li, Y., Chen, W.J., Yang, D., Zhong, G.C., Zhou, H.Z., Ren, C.Y., Yu, H.T. and Ling, H. (2011) Improved expression of secretory and trimeric proteins in mammalian cells via the introduction of a new trimer motif and a mutant of the tPA signal sequence. *Appl. Microbiol. Biotechnol.*, 91(3): 731–740.
97. Kreiter, S., Selmi, A., Diken, M., Sebastian, M., Osterloh, P., Schild, H., Huber, C., Türeci, Ö. and Sahin, U. (2008) Increased antigen presentation efficiency by coupling antigens to MHC Class I trafficking signals. *J. Immunol.*, 180(1): 309–318.
98. Sharp, P.M. and Li, W.H. (1987) The codon adaptation index--a measure of directional synonymous codon usage bias, and its potential applications. *Nucleic Acids Res*., 15(3): 1281–1295.
99. Wayment-Steele, H.K., Kim, D.S., Choe, C.A., Nicol, J.J., Wellington-Oguri, R., Watkins, A.M., Parra Sperberg, R.A., Huang, P.S., Participants, E. and Das, R. (2021) Theoretical basis for stabilizing messenger RNA through secondary structure design. *Nucleic Acids Res.*, 49(18): 10604–10617.
100. Schrom, E., Huber, M., Aneja, M., Dohmen, C., Emrich, D., Geiger, J., Hasenpusch, G., Herrmann-Janson, A., Kretzschmann, V., Mykhailyk, O., Pasewald, T., Oak, P., Hilgendorff, A., Wohlleber, D., Hoymann, H.G., Schaudien, D., Plank, C., Rudolph, C. and Kubisch-Dohmen, R. (2017) Translation of angiotensin-converting enzyme 2 upon liver-and lung-targeted delivery of optimized chemically modified mRNA. *Mol. Ther. Nucleic Acids.*, 7: 350–365.
101. Waggoner, S.A. and Liebhaber, S.A. (2003) Regulation of alpha-globin mRNA stability. *Exp. Biol. Med.* (*Maywood*), 228(4): 387–395.
102. Xia, X. (2021) Detailed dissection and critical evaluation of the Pfizer/BioNTech and moderna mRNA vaccines. *Vaccines* (*Basel*), 9(7): 734.
103. Orlandini von Niessen, A.G., Poleganov, M.A., Rechner, C., Plaschke, A., Kranz, L.M., Fesser, S., Diken, M., Löwer, M., Vallazza, B., Beissert, T., Bukur, V., Kuhn, A.N., Türeci, Ö. and Sahin, U. (2019) Improving mRNA-based therapeutic gene delivery by expression-augmenting 3' UTRs identified by cellular library screening. *Mol. Ther.*, 27(4): 824–836.
104. Volloch, V. and Housman, D. (1981) Stability of globin mRNA in terminally differentiating murine erythroleukemia cells. *Cell*. 23(2): 509–514.
105. Andreev, D.E., Loughran, G., Fedorova, A.D.,

Mikhaylova, M.S., Shatsky, I.N. and Baranov, P.V. (2022) Non-AUG translation initiation in mammals. *Genome Biol.*, 23(1): 111.

106. Holtkamp, S., Kreiter, S., Selmi, A., Simon, P., Koslowski, M., Huber, C., Türeci, O. and Sahin, U. (2006) Modification of antigen-encoding RNA increases stability, translational efficacy, and T-cell stimulatory capacity of dendritic cells. *Blood*, 108(13): 4009–4017.

****